Computers, Materials & Continua CMC, vol.62, no.2, pp.607-629, 2020

Forced Vibration Analysis of Functionally Graded Anisotropic Nanoplates Resting on Winkler/Pasternak-Foundation

Behrouz Karami[1], Maziar Janghorban[1] and Timon Rabczuk[2, *]

Abstract: This study investigates the forced vibration of functionally graded hexagonal nano-size plates for the first time. A quasi-three-dimensional (3D) plate theory including stretching effect is used to model the anisotropic plate as a continuum one where small-scale effects are considered based on nonlocal strain gradient theory. Also, the plate is assumed on a Pasternak foundation in which normal and transverse shear loads are taken into account. The governing equations of motion are obtained via the Hamiltonian principles which are solved using analytical based methods by means of Navier's approximation. The influences of the exponential factor, nonlocal parameter, strain gradient parameter, Pasternak foundation coefficients, length-to-thickness, and length-to-width ratios on the dynamic response of the nanoplates are examined. In addition, the accuracy of an isotropic approximate instead of the anisotropic model is studied. The dynamic behavior of the system shows that mechanical mathematics-based models may get better results considering the anisotropic model because the dynamic response can cause prominent differences (up to 17%) between isotropic approximation and anisotropic model.

Keywords: Functionally graded materials, dynamic deflection, nonlocal train gradient theory, Winkler-Pasternak elastic foundation.

1 Introduction

Forced vibration occurs in different ways in industry. Although it is desirable in some cases such as vibrating conveyors but in most cases it is unpleasant. Different kinds of dynamic forces can act on our system such as impulse loading or harmonic force. Systems under these dynamic loading can have unfavorable and malicious behaviors. Therefore, it is essential to have deep study on this topic. Basically, in studying engineering structures, it is desirable to use the simplest possible methodology with acceptable errors in the results because in engineering unlike some sciences, we are not looking for exact answer. This lack of attention to exact solutions and focus on simple engineering techniques may cause some unacceptable errors in engineering design. One of the possible approximations that may cause inaccurate results is replacing the material properties of anisotropic materials such as triclinic or monoclinic materials with the

[1] Department of Mechanical Engineering, Marvdasht Branch, Islamic Azad University, Marvdasht, Iran.

[2] Institute of Research and Development, Duy Tan University, Da Nang, Viet Nam.

[*] Corresponding Author: Timon Rabczuk. Email: timon.rabczuk@uni-weimar.de.

properties of isotropic ones. Although in several cases this approximation is wisely but it cannot be generalized to all cases. Hence, in the present investigation, we study the accuracy of replacing isotropic approximation for forced vibration of functionally graded materials (FGMs).

FGMs are new class of advanced composite materials in which the properties vary continuously or exponentially along a direction or more. Variable properties along the directions help these types of materials to have the appropriate benefits such as thermal resistance, high strength, etc. together. The mechanism of operation of these materials usually cover for tolerates the acceptable temperature by a phase while the second one gives an expedient mechanical property. Usually two types of FGMs modeling have been studied in the past decades 1) power-law function (P-FGM) 2) exponential function (E-FGM). The operation of different micromechanical schemes to estimate the effective materials properties of FGMs recently developed by Karami et al. [Karami, shahsavari, janghorban et al. (2019)] for free vibration of curved microbeams. Thermo-elastic vibration analysis of FGMs was analyzed by Aria et al. [Aria, Rabczuk and Friswell (2019)] considering isogeometric analysis (IGA). Chen et al. [Chen, Yang and Kitipornchai (2016)] reported the free and forced vibrations of FGM beams including porosity effect. Simsek et al. [Şimşek and Aydın (2017)] studied forced vibration of FGM microplates where the equations were solved in time domain by means of Newmark's method. Static and dynamic deformations of thick FGM plates were proposed by Qian et al. [Qian, Batra and Chen (2004)] using meshless local Petrov-Galerkin method. Applications of three different elastic foundations on free vibration of FGM plate was proposed by Shahsavari et al. [Shahsavari, Shahsavari, Li et al. (2018)] and solved analytically using Galerkin method. Due to its many uses in the coating, military, reactor, turbine, etc., FGM has been much more studied than these previous reviews [Pan (2003); Ramirez, Heyliger and Pan (2006); Song, Kitipornchai and Yang (2017); Barati (2018)]. According to the reviewed studies on the FGMs, there is no study on the forced vibration of E-FGM nano-size plate made of beryllium crystal under a sinusoidal dynamic load even at macro-scale.

Nanotechnology has prominent advantages for developers who are working to make people's lives easier. This relatively new technology has led to the construction of subatomic or nanostructured structures that have a variety of applications in medicine, electronics, mechanics, solar cells, etc. Therefore, in the field of mechanical engineering, the study of the behavior of nanoscale structures has been of great importance. Three different method are suggested to predict the mechanics of these structures (i.e., experimental testes, molecular dynamics (MD) simulation and non-classical theories). Experimental tests and MD simulation have more complexity compared to non-classical theories, which has led to the development of this category of theories in recent years. Because in engineering, reducing the complexity of computing, which leads to time and cost savings, it is important.

Two small-scale dependent non-classical theory was proposed by Askes and Aifantis et al. [Askes and Aifantis (2009)] for the first time. Nonlocal strain gradient theory captures nonlocality and strain gradient size-dependency together by adding two extra parameters on the classical relation. By accounting for both stress and strain gradient effects, this theory

available to have both stiffness softening and hardening mechanism of nanostructures. MD simulation results and the calibration between the results of the mentioned model and experimental data have proved the accuracy and availability of nonlocal strain gradient theory to study the nanostructures. Hence a large number of investigations have been done on the static, dynamic and stability of nano-size particles, beams, plates and shells. Some of them reported in the following: Forced resonant vibration of FG nanoplate was studied by Nami et al. [Nami and Janghorban (2014)] using nonlocal and strain gradient elasticity theory separately. Application of elastic waves in graded nonlocal strain gradient timoshenko beam was proposed by Li et al. [Li, Hu and Ling (2015); Sahmani, Aghdam and Rabczuk (2018)] proposed a non-classical model to study the static response of graphene nanoplatelets reinforced FG microplates including nonlinear terms. Dynamic response of FG nanotube using nonlocal strain gradient theory was reported by Farajpour et al. [Farajpour, Ghayesh and Farokhi (2018)]. It is clear that size-dependent studies of nanostructures using mentioned particular non-classical model are very high, but little research has been done based on nonlocal strain gradient model in sub-atomic structures for anisotropic materials, while no study cover the dynamic deflection of hexagonal nanoplate including Winkler-Pasternak elastic foundation.

In the current work, by adopting a quasi-3D plate model in conjunction with the nonlocal strain gradient theory including two small-scale parameters, the equations of motion are obtained and solved analytically for forced vibration of the nanoplate with all simply-supported edges.

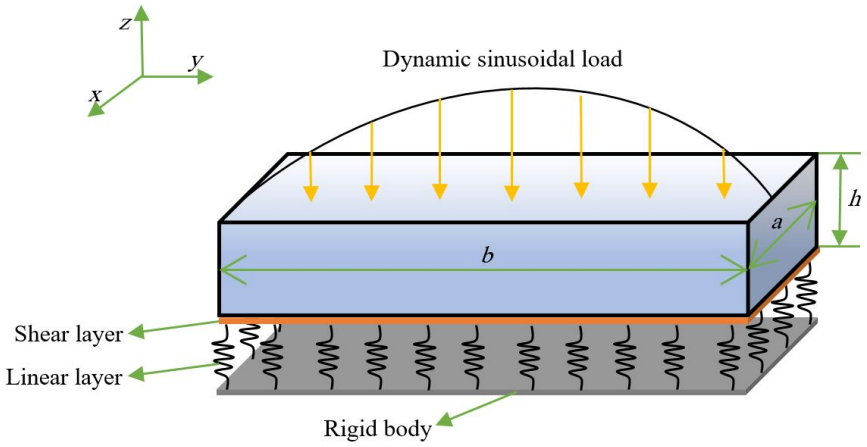

Figure 1: Schematic of FGM anisotropic nanoplates resting on pasternak foundation subjected to dynamic transverse sinusoidal mechanical load

2 Mathematical modeling

In the current work a nano-size plate made of FG anisotropic material is assumed including thickness h, length a and width b (Fig. 1).

2.1 Nonlocal strain gradient theory

For several years, some of the researchers have been used strain gradient theory with one length scale parameter to study different phenomena. This theory had the advantage of simplicity in comparison with several other size-dependent theories although it did not have enough accuracy. In 2009, Askes et al. [Askes and Aifantis (2009)] focused on another size-dependent theory which had two length scale parameters which can be written as below,

$$\left[1-\ell_1^2\nabla^2\right]\sigma_{ij}=Q_{ijkl}\left[1-\ell_2^2\nabla^2\right]\varepsilon_{kl} \tag{1}$$

where ℓ_1 and ℓ_2 denote the scale coefficients whose capture the nonlocality and strain gradient size-dependency, respectively.

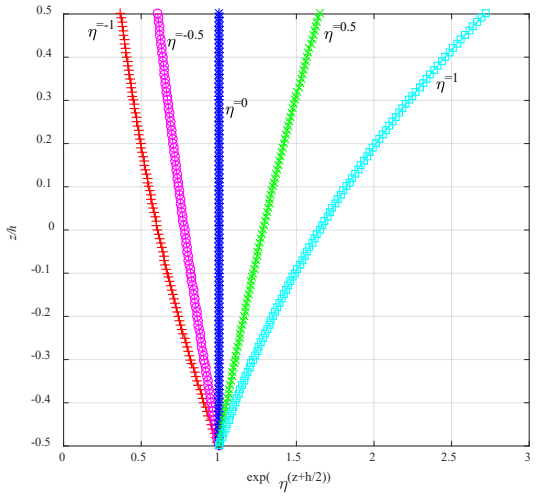

Figure 2: Changing the exponential factor along the z-direction of FG anisotropic nanoplate

2.2 Functionally graded anisotropic materials

For a hexagonal material, the elastic constants are given as [Batra, Qian and Chen (2004)]

$$C_{ij}^0=\begin{bmatrix} 298.2 & 27.7 & 11 & 0 & 0 & 0 \\ & 298.2 & 50.87 & 0 & 0 & 0 \\ & & 340.8 & 0 & 0 & 0 \\ & sym. & & 165.5 & 0 & 0 \\ & & & & 165.5 & 0 \\ & & & & & 135.3 \end{bmatrix}\times GPa \tag{2}$$

Some materials that have been produced in recent decades have been able to open their way to the industry over time. A class of them is FGM that is considered by researchers for their outstanding properties. In this type of material, we are faced with a continuous change in properties such as modulus of elasticity in one of the material directions although recently the variation of properties in more than one direction is also studied. These variations can be occurred in different ways. In this article, exponential variation

for elastic constants is chosen. The following relation proposed by Pan et al. is utilized to estimate the effective material properties of anisotropic materials [Pan (2003)]:

$$Q_{ij} = Q_{ij}^{0} \exp(\eta(z+\frac{h}{2})) \tag{3}$$

in above equation η is the exponential factor which presents the material gradient along the z-direction (see in Fig. 2); η=0 represents the homogenous case, and η<0, η>0 represent, respectively, the graded soft and stiff materials. For an FG anisotropic nanoplate, Eq. (3) is rewritten as:

$$\Re_{\mu}\begin{Bmatrix}\sigma_{xx}\\ \sigma_{yy}\\ \sigma_{zz}\\ \tau_{yz}\\ \tau_{xz}\\ \tau_{y}\end{Bmatrix} = \Re_{\ell}\begin{bmatrix} Q_{11} & Q_{12} & Q_{13} & 0 & 0 & 0\\ & Q_{22} & Q_{23} & 0 & 0 & 0\\ & & Q_{33} & 0 & 0 & 0\\ & & \text{sym.} & Q_{44} & 0 & 0\\ & & & & C_{55} & 0\\ & & & & & C_{66}\end{bmatrix}\begin{Bmatrix}\varepsilon_{xx}\\ \varepsilon_{yy}\\ \varepsilon_{zz}\\ \gamma_{yz}\\ \gamma_{xz}\\ \gamma_{xy}\end{Bmatrix} \tag{4}$$

where

$$\Re_{\mu} = \left[1-\mu\nabla^{2}\right], \Re_{\ell} = \left[1-\lambda\nabla^{2}\right] \tag{5}$$

herein $\mu = \ell_1^2$ and $\lambda = \ell_2^2$. According to the isotropic approximation, the following relation are presented to examine the effective material properties of the FG nanoplate as below:

$$\begin{aligned} Q_{11}^{0} = Q_{22}^{0} = Q_{33}^{0} &= \frac{(1-\upsilon)E}{(1-2\nu)(1+\nu)}\\ Q_{12}^{0} = Q_{13}^{0} = Q_{23}^{0} &= \frac{\nu E}{(1-2\nu)(1+\nu)}\\ Q_{44}^{0} = Q_{55}^{0} = Q_{66}^{0} &= \frac{E}{2(1+\nu)} \end{aligned} \tag{6}$$

in which the Young's modulus and Poisson's ratio of the beryllium crystal are approximated as E=287 GPa ν=0.32, respectively, and the density is ρ=1850 kg/m^3 [Batra, Qian and Chen (2004)].

2.3 Kinematics

İn the current work a five-unkown dependent refined plate model is utilized in which the in-plane and out of plane displacements are defined as below

$$\begin{aligned} u(x,y,z,t) &= u_0(x,y,t) - z\frac{\partial w_b}{\partial x} - f(z)\frac{\partial w_s}{\partial x}\\ v(x,y,z,t) &= v_0(x,y,t) - z\frac{\partial w_b}{\partial y} - f(z)\frac{\partial w_s}{\partial y}\\ w(x,y,z,t) &= w_b(x,y,t) + w_s(x,y,t) + g(z)\varphi(x,y,t) \end{aligned} \tag{7}$$

herein u, v and w denote the displacements along the x, y and z-direction, respectively; $f(z)$ is a shape function which must be tending the shear strains at the top and bottom surfaces of the studied plate to zero and is defined as below:

$$f(z) = -\frac{z}{4} + \frac{5z^3}{3h^2} \tag{8}$$

where

$$g(z) = 1 - \frac{\partial f(z)}{\partial z} \tag{9}$$

According to the mentioned displacement field (Eq. (7)), the non-zero strains are expressed as below:

$$\begin{Bmatrix} \varepsilon_x \\ \varepsilon_y \\ \gamma_{xy} \end{Bmatrix} = \begin{Bmatrix} \varepsilon_x^0 \\ \varepsilon_y^0 \\ \gamma_{xy}^0 \end{Bmatrix} + z \begin{Bmatrix} k_x^b \\ k_y^b \\ k_{xx}^b \end{Bmatrix} + f(z) \begin{Bmatrix} k_x^s \\ k_y^s \\ k_{xx}^s \end{Bmatrix}, \begin{Bmatrix} \gamma_{yz} \\ \gamma_{xz} \end{Bmatrix} = g(z) \begin{Bmatrix} \gamma_{yz}^0 \\ \gamma_{xz}^0 \end{Bmatrix}, \varepsilon_z = \frac{\partial g(z)}{\partial z} \varepsilon_z^0 \tag{10}$$

where

$$\begin{Bmatrix} \varepsilon_{xx}^0 \\ \varepsilon_{yy}^0 \\ \gamma_{xy}^0 \end{Bmatrix} = \begin{Bmatrix} \dfrac{\partial u_0}{\partial x} \\ \dfrac{\partial v_0}{\partial y} \\ \dfrac{\partial u_0}{\partial y} + \dfrac{\partial v_0}{\partial x} \end{Bmatrix}, \begin{Bmatrix} k_{xx}^b \\ k_{yy}^b \\ k_{xx}^b \end{Bmatrix} = \begin{Bmatrix} -\dfrac{\partial^2 w_b}{\partial x^2} \\ -\dfrac{\partial^2 w_b}{\partial y^2} \\ -2\dfrac{\partial^2 w_b}{\partial x \partial y} \end{Bmatrix}, \begin{Bmatrix} k_{xx}^s \\ k_{yy}^s \\ k_{xx}^s \end{Bmatrix} = \begin{Bmatrix} -\dfrac{\partial^2 w_s}{\partial x^2} \\ -\dfrac{\partial^2 w_s}{\partial y^2} \\ -2\dfrac{\partial^2 w_s}{\partial x \partial y} \end{Bmatrix} \tag{11}$$

$$\begin{bmatrix} \gamma_{yz}^0 \\ \gamma_{xz}^0 \end{bmatrix} = \begin{Bmatrix} \dfrac{\partial w_s}{\partial y} + \dfrac{\partial \varphi_z}{\partial y} \\ \dfrac{\partial w_s}{\partial x} + \dfrac{\partial \varphi_z}{\partial x} \end{Bmatrix}, \varepsilon_z^0 = \varphi_z$$

2.4 Equations of motion

The Hamilton's principle is adopted as

$$\int_0^t \delta(U - K + V) dt = 0 \tag{12}$$

in which U is strain energy, K indicate the kinetic energy and V denotes the work done by applied forces. The first variation of strain energy can be written as

$$\begin{aligned} \delta U &= \int_{-h/2}^{h/2} \int_A \left[\sigma_x \delta\varepsilon_x + \sigma_y \delta\varepsilon_y + \sigma_z \delta\varepsilon_z + \tau_{yz} \varepsilon_{yz} + \tau_{xz} \varepsilon_{xz} + \tau_{xy} \varepsilon_{xy} \right] dA\, dz \\ &= \int_A \left[N_x \delta\varepsilon_x^0 + N_y \delta\varepsilon_y^0 + N_z \delta\varepsilon_z^0 + N_{xy} \delta\gamma_{xy}^0 + M_x^b \delta k_x^b + M_y^b \delta k_y^b + M_{xy}^b \delta k_{xy}^b \right. \\ &\left. + M_x^s \delta k_x^s + M_y^s \delta k_y^s + M_{xy}^s \delta k_{xy}^s + Q_{yz}^s \gamma_{yz}^0 + Q_{xz}^s \gamma_{xz}^0 \right] dA = 0 \end{aligned} \tag{13}$$

in above relation the stress resultants (N, M, and Q) are expressed by:

$$N_{ij} = \int_{-h/2}^{h/2} \sigma_{ij} dz \ : (i, j = x, y) \tag{14}$$

$$N_z = \int_{-h/2}^{h/2} \frac{\partial g(z)}{\partial z} \sigma_z dz$$

$$(M_{ij}^b, M_{ij}^s) = \int_{-h/2}^{h/2} (z, f(z)) \sigma_{ij} dz \ : (i, j = x, y)$$

$$(Q_{xz}^s, Q_{yz}^s) \int_{-h/2}^{h/2} g(z)(\tau_{xz}, \tau_{yz}) dz$$

The first variation of kinetic energy is defined as follows

$$\begin{aligned} \delta K &= \int_{-h/2}^{h/2} \int_A \left[\dot{u}_0 \delta \dot{u}_0 + \dot{v}_0 \delta \dot{v}_0 + \dot{w} \, \delta \dot{w} \right] dA \, dz \\ &= \int_A \Big\{ I_0 \left(\dot{u}_0 \delta \dot{u}_0 + \dot{v}_0 \delta \dot{v}_0 + (\dot{w}_b + \dot{w}_s)(\delta \dot{w}_b + \delta \dot{w}_s) \right) \\ &- I_1 \left(\dot{u}_0 \frac{\partial \delta \dot{w}_b}{\partial x} + \frac{\partial \dot{w}_b}{\partial x} \delta \dot{u}_0 + \dot{v}_0 \frac{\partial \delta \dot{w}_s}{\partial y} + \frac{\partial \dot{w}_s}{\partial y} \delta \dot{v}_0 \right) \\ &- J_1 \left(\dot{u}_0 \frac{\partial \delta \dot{w}_s}{\partial x} + \frac{\partial \dot{w}_s}{\partial x} \delta \dot{u}_0 + \dot{v}_0 \frac{\partial \delta \dot{w}_s}{\partial y} + \frac{\partial \dot{w}_s}{\partial y} \delta \dot{v}_0 \right) \\ &+ I_2 \left(\frac{\partial \delta \dot{w}_b}{\partial x} \frac{\partial \delta \dot{w}_b}{\partial x} + \frac{\partial \delta \dot{w}_b}{\partial y} \frac{\partial \delta \dot{w}_b}{\partial y} \right) + K_2 \left(\frac{\partial \delta \dot{w}_s}{\partial x} \frac{\partial \delta \dot{w}_s}{\partial x} + \frac{\partial \delta \dot{w}_s}{\partial y} \frac{\partial \delta \dot{w}_s}{\partial y} \right) \\ &+ J_2 \left(\frac{\partial \dot{w}_b}{\partial x} \frac{\partial \delta \dot{w}_s}{\partial x} + \frac{\partial \dot{w}_s}{\partial x} \frac{\partial \delta \dot{w}_b}{\partial x} + \frac{\partial \dot{w}_b}{\partial y} \frac{\partial \delta \dot{w}_s}{\partial y} + \frac{\partial \dot{w}_s}{\partial y} \frac{\partial \delta \dot{w}_b}{\partial y} \right) \\ &+ J_1^s \left((\dot{w}_b + \dot{w}_s) \delta \dot{\varphi} + \dot{\varphi} \delta (\dot{w}_b + \dot{w}_s) \right) + K_2^s \dot{\varphi} \delta \dot{\varphi} \Big\} dA \end{aligned} \tag{15}$$

herein

$$\left\{ I_0, I_1, J_1, J_1^s, I_2, J_2, K_2, K_2^s \right\} = \int_{-h/2}^{h/2} \left\{ 1, z, f, g, z^2, zf, f^2, g^2(z) \right\} \rho(z) dz \tag{16}$$

The first variation of work done by external forces can be approximated as:

$$\delta V = -\int_0^a \int_0^b q \, \delta(w) dy dx \tag{17}$$

in which q denotes the distributed transverse load. By inserting Eqs. (13), (15) and (17) into Eq. (12), the following equilibrium equations are obtained:

$$\delta u_0 : \frac{\partial N_x}{\partial x} + \frac{\partial N_{xy}}{\partial y} = I_0 \ddot{u}_0 - I_1 \frac{\partial \ddot{w}_b}{\partial x} - J_1 \frac{\partial \ddot{w}_s}{\partial x} \tag{18}$$

$$\delta v_0 : \frac{\partial N_{xy}}{\partial x} + \frac{\partial N_y}{\partial y} = I_0 \ddot{v}_0 - I_1 \frac{\partial \ddot{w}_b}{\partial y} - J_1 \frac{\partial \ddot{w}_s}{\partial y} \tag{19}$$

$$\begin{aligned} \delta w_b : &\frac{\partial^2 M_x^b}{\partial x^2} + 2 \frac{\partial^2 M_{xy}^b}{\partial x \partial y} + \frac{\partial^2 M_y^b}{\partial y^2} - q = I_0 \left(\ddot{w}_b + \ddot{w}_s \right) + I_1 \left(\frac{\partial \ddot{u}_0}{\partial x} + \frac{\partial \ddot{v}_0}{\partial y} \right) \\ &- I_2 \nabla^2 \ddot{w}_b - J_2 \nabla^2 \ddot{w}_s + J_1^s \ddot{\varphi} \end{aligned} \tag{20}$$

$$\delta w_s : \frac{\partial^2 M_x^s}{\partial x^2} + 2\frac{\partial^2 M_{xy}^s}{\partial x \partial y} + \frac{\partial^2 M_y^s}{\partial y^2} + \frac{\partial Q_{xz}^s}{\partial x} + \frac{\partial Q_{yz}^s}{\partial y} - q = I_0\left(\ddot{w}_b + \ddot{w}_s\right) \tag{21}$$
$$+J_1\left(\frac{\partial \ddot{u}_0}{\partial x} + \frac{\partial \ddot{v}_0}{\partial y}\right) - J_2\nabla^2\ddot{w}_b - K_2\nabla^2\ddot{w}_s + J_1^s\ddot{\varphi}$$

$$\delta\varphi : \frac{\partial Q_{xz}^s}{\partial x} + \frac{\partial Q_{yz}^s}{\partial y} - (N_z + q) = J_1^s\left(\ddot{w}_b + \ddot{w}_s\right) - K_2^s\ddot{\varphi} \tag{22}$$

The governing equations of motion in terms of the displacements for a nanoplate considering all independent elastic components are expressed by inserting Eq. (14) into Eqs. (18)-(22) which are reported in the appendix.

3 Solution procedure

The Navire method is employed here to solve the governing equations for FG hexagonal nanoplate including simply-supported edges as follow,

$$u_0 = \sum_{m=1}^{\infty}\sum_{n=1}^{\infty} U_{mn}\cos(\alpha x)\sin(\beta y)\sin\Omega t \tag{23}$$

$$v_0 = \sum_{m=1}^{\infty}\sum_{n=1}^{\infty} V_{mn}\sin(\alpha x)\cos(\beta y)\sin\Omega t \tag{24}$$

$$w_b = \sum_{m=1}^{\infty}\sum_{n=1}^{\infty} W_{bmn}\sin(\alpha x)\sin(\beta y)\sin\Omega t \tag{25}$$

$$W_s = \sum_{m=1}^{\infty}\sum_{n=1}^{\infty} W_{smn}\sin(\alpha x)\sin(\beta y)\sin\Omega t \tag{26}$$

$$w_{st} = \sum_{m=1}^{\infty}\sum_{n=1}^{\infty} W_{stmn}\sin(\alpha x)\sin(\beta y)\sin\Omega t \tag{27}$$

$$q = \sum_{m=1}^{\infty}\sum_{n=1}^{\infty} Q_{mn}\sin(\alpha x)\sin(\beta y)\sin\Omega t \tag{28}$$

where $\alpha=m\pi/a$, $\beta=n\pi/b$. The simply-supported boundary conditions using the present plate model are defined as below:

$$w_b = w_s = 0$$
$$\frac{\partial^2 w_b}{\partial x^2} = \frac{\partial^2 w_s}{\partial x^2} = \frac{\partial^2 w_b}{\partial y^2} = \frac{\partial^2 w_s}{\partial y^2} = 0 \tag{29}$$
$$\frac{\partial^4 w_b}{\partial x^4} = \frac{\partial^4 w_s}{\partial x^4} = \frac{\partial^4 w_b}{\partial y^4} = \frac{\partial^4 w_s}{\partial y^4} = 0$$

By using the aforementioned method, the matrix form for the solution of forced vibration of the nanoplates can be expressed as,

$$[K]X = [F] \tag{30}$$

in which [K] indicates the stiffness matrix. It is important to noted that, the weakness of the present solution procure is inability to solve the arbitrary boundary conditions and all independent elastic constants for the nanoplates. Hence the numerical based methods such as differential quadrature method, finite element analysis, IGA, etc. are suggested to solve the present model for different anisotropic materials such as triclinic material and different boundary conditions.

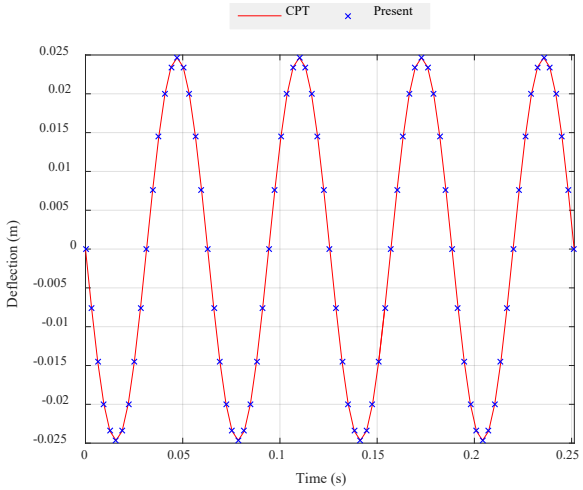

Figure 3: Comparison of the present model with the results of nonlocal strain gradient classical plate model (E=380 GPa, ρ=2370 kg/m^3, v=0.3, a=10, a/h=100, μ=λ=1)

4 Numerical results

In this section, the numerical results for the forced vibration of rectangular nanoplates made of FG anisotropic material on the basis of a quasi-3D plate model in conjunction with the general nonlocal strain gradient theory are presented. As the first example, in Fig. 3, the dynamic deflection of simply supported rectangular nanoplates under sinusoidal loading is discussed based on present methodology and classical plate theory (CPT). From this figure, one can find the accuracy of present method. It can be seen that our numerical results predict the deflection correctly.

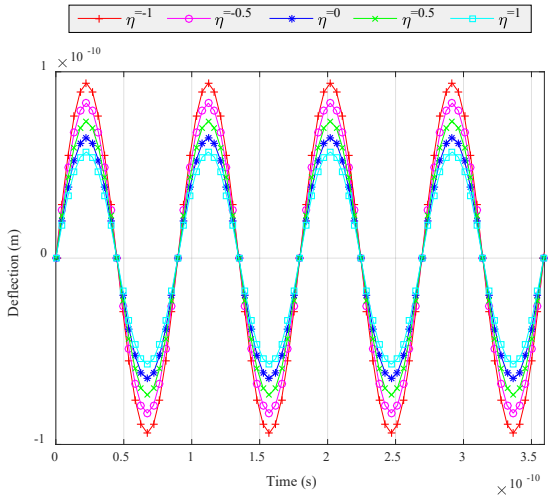

Figure 4: Time variation of transverse motion of FG anisotropic nanoplates considering exponential factor, (a=10 nm, a/h=20, μ=λ=1 nm^2)

In Fig. 4 the deflections of a specific point versus time for FG anisotropic nanoplate subjected to sinusoidal loading including both nonlocal and gradient parameters are studied. In this figure, different types of FG anisotropic nanoplate are considered by changing the exponential factor from negative to positive numbers. The sinusoidal behavior of nanoplate may be predictable because of our engineering sense of a macro plate under sinusoidal loading. This figure shows that with the increase of exponential factor from negative values to positive ones, the deflections are decrease. From this conclusion one can find that increasing the exponential factor will cause increment in the stiffness of FG anisotropic nanoplates.

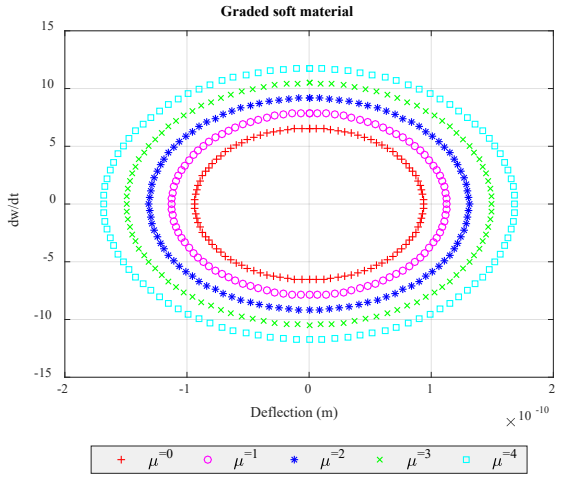

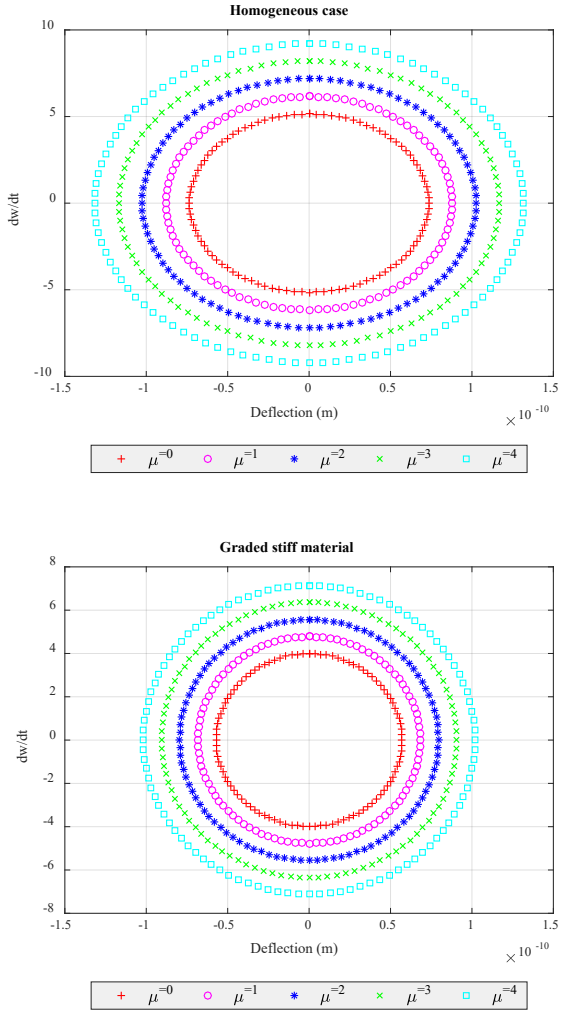

Figure 5: The effects of nonlocal parameter on the phase plots vs. deflection for the forced vibration of FG anisotropic nanoplates, (a=10 nm, a/h=20, λ=0 nm^2)

Fig. 5 depicts the variations of deflections versus the rate of deflections, known as phase plot considering nonlocal parameter. In this figure, three types of FG anisotropic materials are studied: 1-Graded soft material (negative exponential factor) 2-Homogenous material (zero exponential factor) 3-Graded stiff material (positive exponential factor). For first two types some elliptical behaviors can be seen but for the third one, circular behavior is achieved. This conclusion is independent of the value of nonlocal parameter. In addition, by increasing the nonlocal parameter, both elliptical and circular paths become larger. It is important to note that from the knowledge of authors, these shapes are not unchangeable. With changing the number of studied points some

other shapes may be achieved. Therefore, in this figure we do not draw lines and we only use points to show the results.

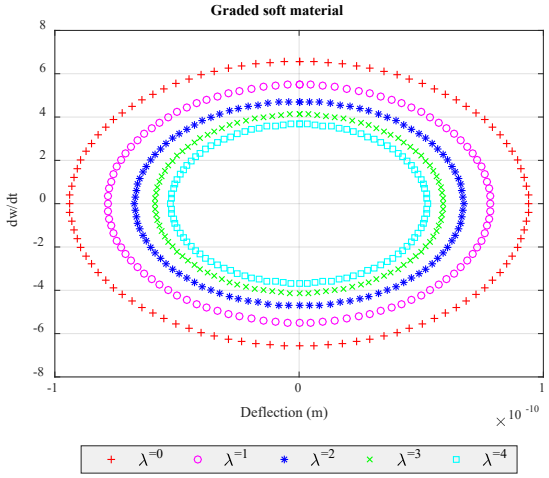

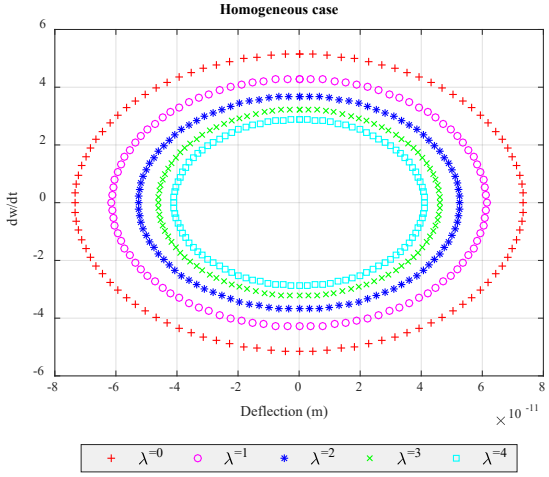

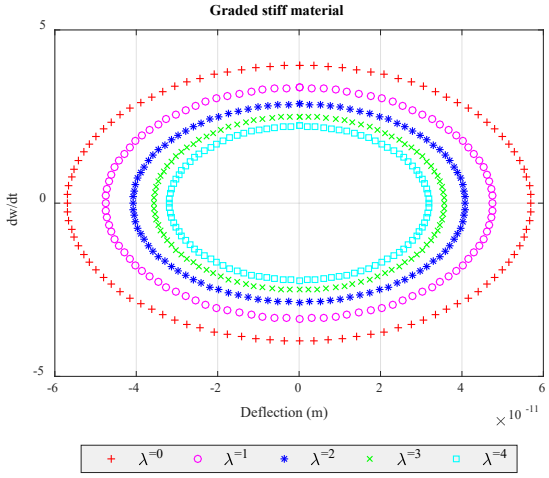

Figure 6: The effects of strain gradient parameter on the phase plots vs. deflection for the forced vibration of FG anisotropic nanoplates, (a=10 nm, a/h=20, μ=0 nm^2)

Phase plot *vs.* deflection for forced vibration of FG anisotropic nanoplates is illustrated in Fig. 6 for different strain gradient parameters. Also, this figure covered the behavior of three types of graded anisotropic materials. As it is seen, by increasing the strain gradient parameter, the elliptical path becomes smaller. This conclusion does not depend on the type of FG anisotropic nanoplate. From this figure, it may be found that for the strain gradient parameters more than 4, the results can be assumed to be constant with a good approximation.

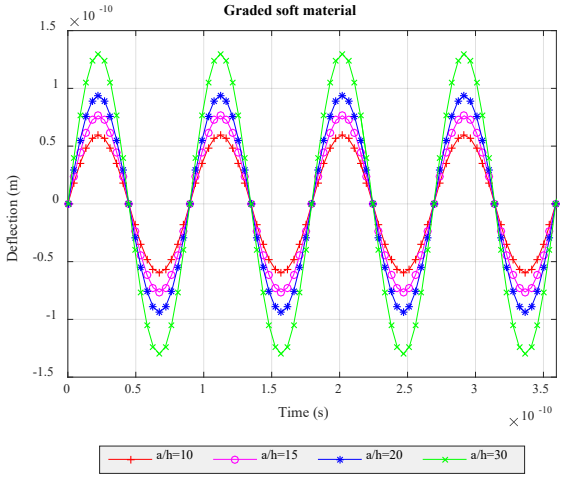

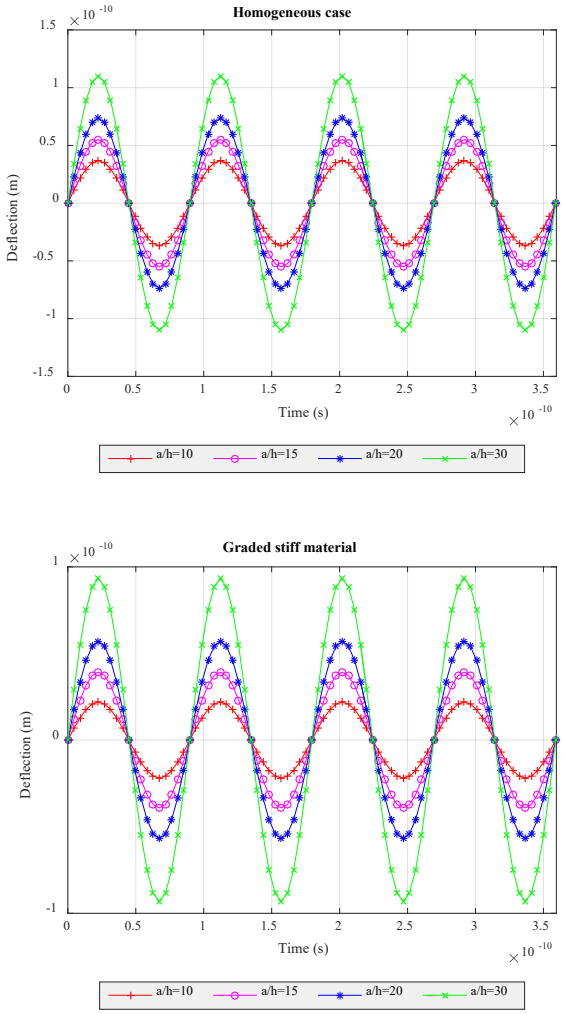

Figure 7: Time variation of transverse motion of FG anisotropic nanoplates considering length-to-thickness ratio, (a=10 nm, μ=λ=1 nm^2)

Fig. 7 shows the effect of length-to-thickness ratio on the time variation of transverse motion of homogenous as well as both soft and stiff grade anisotropic nanoplates. It can be seen that thicker nanoplates have smaller amplitude of the transverse vibration compered to thinner ones. It means that increasing the length-to-thickness ratio increases the deflection of the nanoplates. This conclusion is independent of type of material.

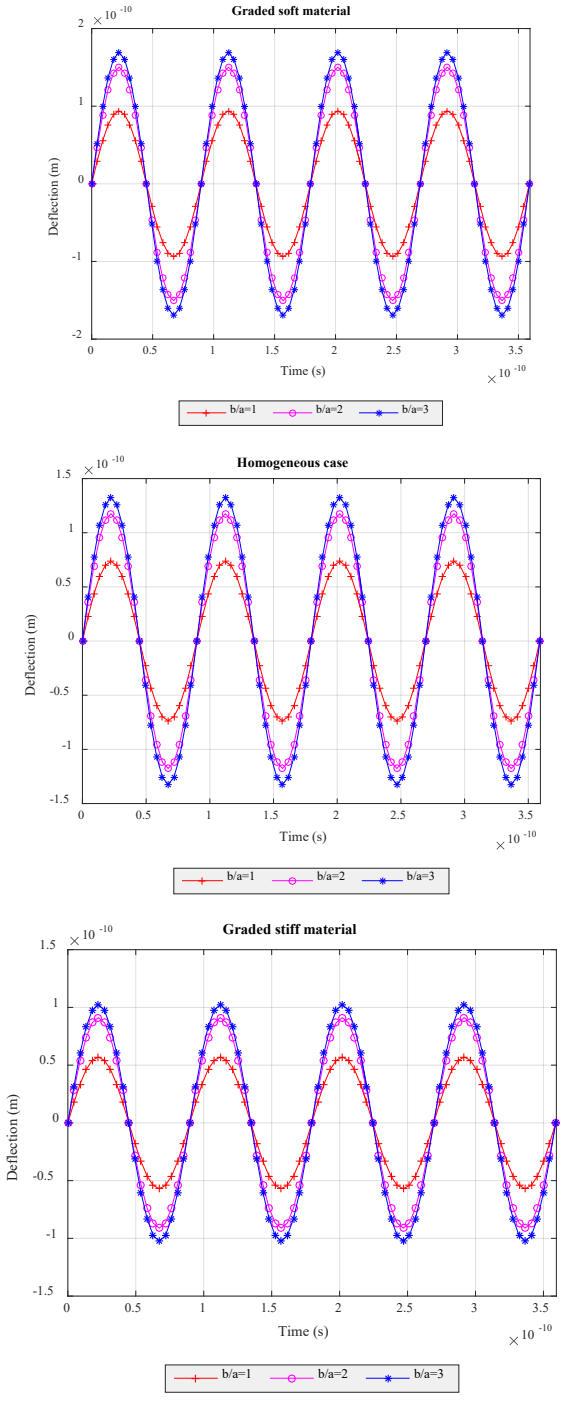

Figure 8: Time variation of transverse motion of FG anisotropic nanoplates considering width-to-length ratio (a=10 nm, a/h=20, $\mu=\lambda$=1 nm^2)

The effect of width-to-length ratio on the time variation of transverse motion of FG anisotropic nanoplate as well as homogenous one is plotted in Fig. 8. It has been observed that square nanoplates (b/a=1) have a smaller deflection than the rectangular ones (b/a>1). In other words, increasing the width-to-length ratio will lead to an increment in the dynamic deflection. From this figure, it may be found that for the width-to-length ratio more than 3, the results can be assumed to be constant with a good approximation. Again, this observation dose not depends on exponential factor values.

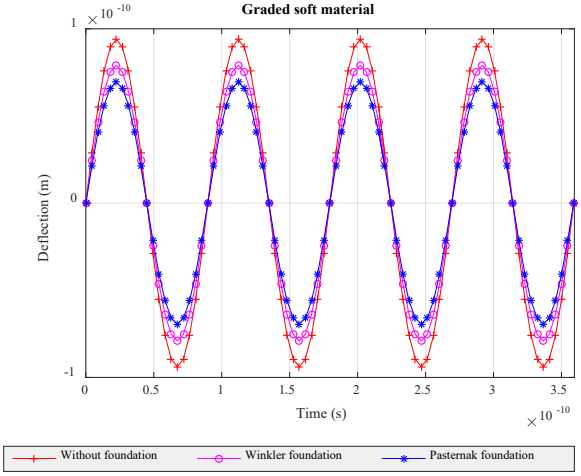

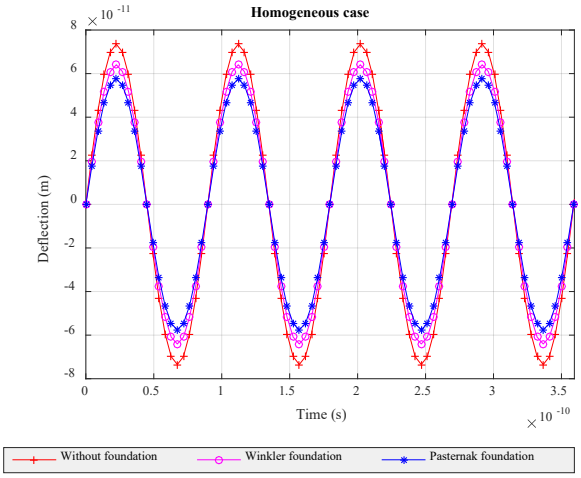

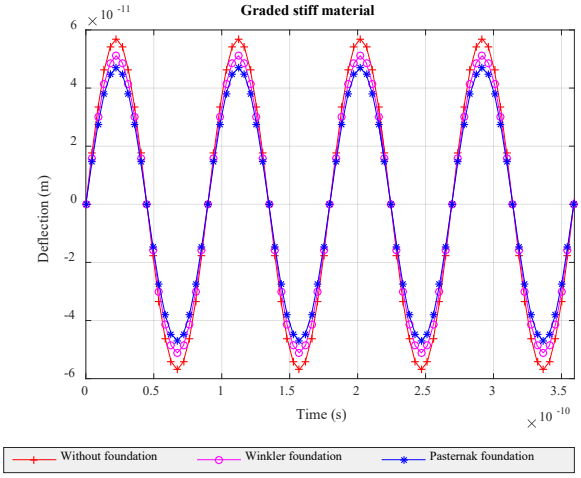

Figure 9: Time variation of transverse motion of FG anisotropic nanoplates *vs.* the effect of elastic foundation (a=10 nm, a/h=20, k_W=2×10^{16} N/m^3, k_P=9 N/m, μ=λ=1 nm^2)

Fig. 9 presents the influence of elastic foundation on the time variation of transverse motion of nanoplates including homogenous, soft and stiff graded type of anisotropic material. As can be seen considering elastic foundation can decrease the dynamic deflection of the system under the sinusoidal loading. It is revealed that the greatest deflection of the nanoplates is obtained for the plate without foundation followed by Winkler foundation, and Pasternak foundation, respectively. Note that, the Winkler foundation only includes linear layer of elastic foundation while the Pasternak one includes both linear and shear layer of elastic foundation.

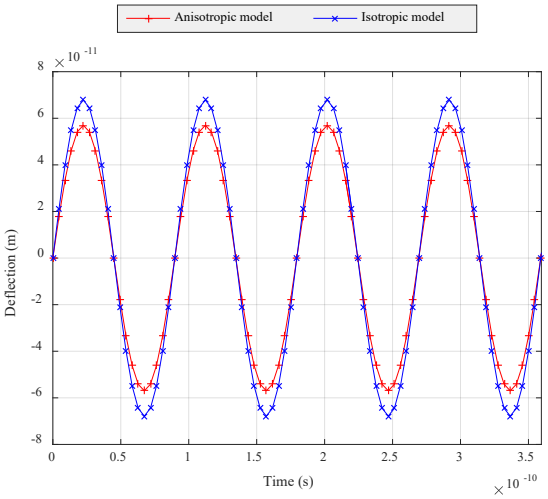

Figure 10: Time variation of transverse motion of stiff graded anisotropic nanoplates including the isotropic and anisotropic approaches (a=10 nm, a/h=20, η=1, μ=λ=1 nm^2)

The accuracy of replacing isotropic approximation for material properties instead of anisotropic one for time variation of transverse motion of stiff graded nanoplate is studied and the results are plotted in Fig. 10. This figure shows a prominent difference between the two approaches that it maybe shows that it is better to model the structures with anisotropic nature. To have a better understanding of this issue phase plot *vs.* deflection for forced vibration of homogenous and graded anisotropic nanoplates is illustrated in Fig. 11 for both models.

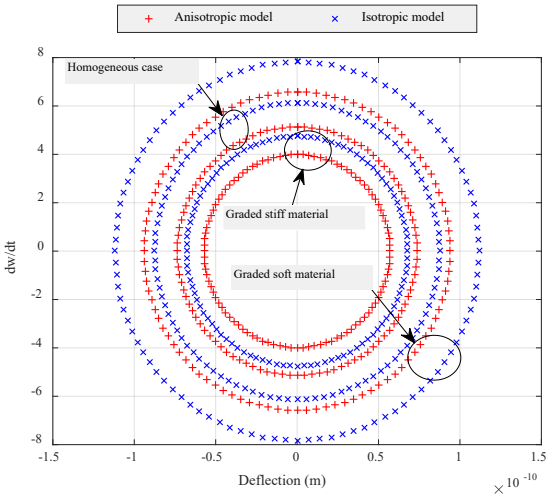

Figure 11: Phase plot *vs.* deflection of FG anisotropic nanoplates including the isotropic and anisotropic approaches (a=10 nm, a/h=20, μ=λ=1 nm^2)

In Fig. 11, a comparison between anisotropic and isotropic models is made including nonlocal and strain gradient parameters. As it can be seen in this figure, significant differences between the results are achieved. Although these differences may be predictable for graded stiff/soft materials because of the influences of power index in FG anisotropic materials but the existence of differences for homogenous case attracts attention to itself. Another interesting point is that these differences are occurred in all studied deflections so one may see the inaccuracy of isotropic model especially for graded soft materials.

5 Conclusions

The essence of the current work lies in the development of a quasi-3D nonlocal strain gradient model for forced vibration analysis of nano-size plates made of FG anisotropic materials. The nanoplates is resting on Winkler-Pasternak elastic foundation. The governing equations and boundary conditions are obtained using Hamilton's principle and solved analytically for all simply-supported edges. The numerical illustrations concern the dynamic deflections of homogenous, soft and stiff graded anisotropic nanoplates including small-scaling parameters. The numerical results reveal that the elastic foundation can decrease the deflection of the system under the sinusoidal loading. Also, increasing the nonlocal parameter decreases the stiffness of the plate that leads to

an increment on the deflection while the opposite behavior is reported for increasing the strain gradient parameter. Furthermore, increasing the exponential factor from negative value to positive one decreases the dynamic deflection of the nanoplates. In other words, that the greatest deflection of the nanoplates is observed for the soft graded nanoplate followed by homogenous nanoplate, and stiff graded nanoplate, respectively. In addition, the dynamic deflection of the nanoplate decreases by increasing the length-to-thickness ratio and the square nanoplates have a smaller amplitude of vibration compared to rectangular ones.

Conflicts of Interest: The authors declare that they have no conflicts of interest to report regarding the present study.

References

Aria, A. I.; Rabczuk, T.; Friswell, M. I. (2019): A finite element model for the thermo-elastic analysis of functionally graded porous nanobeams. *European Journal of Mechanics-A/Solids*, vol. 77, 103767.

Askes, H.; Aifantis, E. C. (2009): Gradient elasticity and flexural wave dispersion in carbon nanotubes. *Physical Review B*, vol. 80, no.19, pp. 195412.

Barati, M. R. (2018): A general nonlocal stress-strain gradient theory for forced vibration analysis of heterogeneous porous nanoplates. *European Journal of Mechanics-A/Solids*, vol.67, pp. 215-230.

Batra, R.; Qian, L.; Chen, L. (2004): Natural frequencies of thick square plates made of orthotropic, trigonal, monoclinic, hexagonal and triclinic materials. *Journal of Sound and Vibration*, vol. 270, no. 4, pp. 1074-1086.

Chen, D.; Yang, J.; Kitipornchai, S. (2016): Free and forced vibrations of shear deformable functionally graded porous beams. *International Journal of Mechanical Sciences*, vol. 108, pp. 14-22.

Farajpour, A.; Ghayesh, M. H.; Farokhi, H. (2018): Large-amplitude coupled scale-dependent behaviour of geometrically imperfect NSGT nanotubes. *International Journal of Mechanical Sciences*, vol. 150, pp. 510-525.

Karami, B.; shahsavari, D.; Janghorban, M.; Li, L. (2019): Influence of homogenization schemes on vibration of functionally graded curved microbeams. *Composite Structures*, vol. 216, pp. 67-79.

Li, L.; Hu, Y.; Ling, L. (2015): Flexural wave propagation in small-scaled functionally graded beams via a nonlocal strain gradient theory. *Composite Structures*, vol. 133, pp. 1079-1092.

Nami, M. R.; Janghorban, M. (2014): Resonance behavior of FG rectangular micro/nano plate based on nonlocal elasticity theory and strain gradient theory with one gradient constant. *Composite Structures*, vol. 111, pp. 349-353.

Pan, E. (2003): Exact solution for functionally graded anisotropic elastic composite laminates. *Journal of Composite materials*, vol. 37, no. 21, pp. 1903-1920.

Qian, L.; Batra, R.; Chen, L. (2004): Static and dynamic deformations of thick functionally graded elastic plates by using higher-order shear and normal deformable plate theory and meshless local Petrov-Galerkin method. *Composites Part B: Engineering*, vol. 35, no. 6-8, pp. 685-697.

Ramirez, F.; Heyliger, P. R.; Pan, E. (2006): Static analysis of functionally graded elastic anisotropic plates using a discrete layer approach. *Composites Part B: Engineering*, vol. 37, no. 1, pp. 10-20.

Sahmani, S.; Aghdam, M. M.; Rabczuk, T. (2018): Nonlinear bending of functionally graded porous micro/nano-beams reinforced with graphene platelets based upon nonlocal strain gradient theory. *Composite Structures*, vol. 186, pp. 68-78.

Shahsavari, D.; Shahsavari, M.; Li, L.; Karami, B. (2018): A novel quasi-3D hyperbolic theory for free vibration of FG plates with porosities resting on Winkler/Pasternak/Kerr foundation. *Aerospace Science and Technology*, vol. 72, pp. 134-149.

Şimşek, M.; Aydın, M. (2017): Size-dependent forced vibration of an imperfect functionally graded (FG) microplate with porosities subjected to a moving load using the modified couple stress theory. *Composite Structures*, vol. 160, pp. 408-421.

Song, M.; Kitipornchai, S.; Yang, J. (2017): Free and forced vibrations of functionally graded polymer composite plates reinforced with graphene nanoplatelets. *Composite Structures*, vol. 159, pp. 579-588.

Appendix

$$\begin{aligned}
&\Re_\ell(A_{11}^1\frac{\partial^2 u_0}{\partial x^2}-B_{11}^1\frac{\partial^3 w_b}{\partial x^3}-C_{11}^1\frac{\partial^3 w_s}{\partial x^3}+A_{12}^1\frac{\partial^2 v_0}{\partial x\partial y}-B_{12}^1\frac{\partial^3 w_b}{\partial x\partial y^2}-C_{12}^1\frac{\partial^3 w_s}{\partial x\partial y^2}+D_{13}^1\frac{\partial\varphi_z}{\partial x})\\
&+\Re_\ell(E_{14}^1(\frac{\partial^2 w_s}{\partial x\partial y}+\frac{\partial^2\varphi_z}{\partial x\partial y})+E_{15}^1(\frac{\partial^2 w_s}{\partial x^2}+\frac{\partial^2\varphi_z}{\partial x^2})+A_{16}^1(\frac{\partial^2 u_0}{\partial x\partial y}+\frac{\partial^2 v_0}{\partial x^2})-2B_{16}^1\frac{\partial^3 w_b}{\partial x^2\partial y}-2C_{16}^1\frac{\partial^3 w_s}{\partial x^2\partial y})\\
&+\Re_\ell(A_{61}^1\frac{\partial^2 u_0}{\partial x\partial y}-B_{61}^1\frac{\partial^3 w_b}{\partial x^2\partial y}-C_{61}^1\frac{\partial^3 w_s}{\partial x^2\partial y}+A_{62}^1\frac{\partial^2 v_0}{\partial y^2}-B_{62}^1\frac{\partial^3 w_b}{\partial y^3}-C_{62}^1\frac{\partial^3 w_s}{\partial y^3}+D_{63}^1\frac{\partial\varphi_z}{\partial y})\\
&+\Re_\ell(E_{64}^1(\frac{\partial^2 w_s}{\partial y^2}+\frac{\partial^2\varphi_z}{\partial y^2})+E_{65}^1(\frac{\partial^2 w_s}{\partial x\partial y}+\frac{\partial^2\varphi_z}{\partial x\partial y})+A_{66}^1(\frac{\partial^2 u_0}{\partial y^2}+\frac{\partial v_0}{\partial x\partial y})-2B_{66}^1\frac{\partial^3 w_b}{\partial x\partial y^2}-2C_{66}^1\frac{\partial^3 w_s}{\partial x\partial y^2})\\
&=\Re_\mu(I_0\frac{\partial^2 u_0}{\partial t^2}-I_1\frac{\partial^3 w_b}{\partial x\partial t^2}-J_1\frac{\partial^3 w_s}{\partial x\partial t^2})
\end{aligned}\tag{A1}$$

$$\begin{aligned}
&\Re_\ell(A_{61}^1\frac{\partial^2 u_0}{\partial x^2}-B_{61}^1\frac{\partial^3 w_b}{\partial x^3}-C_{61}^1\frac{\partial^3 w_s}{\partial x^3}+A_{62}^1\frac{\partial^2 v_0}{\partial x\partial y}-B_{62}^1\frac{\partial^3 w_b}{\partial x\partial y^2}-C_{62}^1\frac{\partial^3 w_s}{\partial x\partial y^2}+D_{63}^1\frac{\partial\varphi_z}{\partial x})\\
&+\Re_\ell(E_{64}^1(\frac{\partial^2 w_s}{\partial x\partial y}+\frac{\partial^2\varphi_z}{\partial x\partial y})+E_{65}^1(\frac{\partial^2 w_s}{\partial x^2}+\frac{\partial^2\varphi_z}{\partial x^2})+A_{66}^1(\frac{\partial^2 u_0}{\partial x\partial y}+\frac{\partial^2 v_0}{\partial x^2})-2B_{66}^1\frac{\partial^3 w_b}{\partial x^2\partial y}-2C_{66}^1\\
&+\Re_\ell(A_{21}^1\frac{\partial^2 u_0}{\partial x\partial y}-B_{21}^1\frac{\partial^3 w_b}{\partial x^2\partial y}-C_{21}^1\frac{\partial^3 w_s}{\partial x^2\partial y}+A_{22}^1\frac{\partial^2 v_0}{\partial y^2}-B_{22}^1\frac{\partial^3 w_b}{\partial y^3}-C_{22}^1\frac{\partial^3 w_s}{\partial y^3}+D_{23}^1\frac{\partial\varphi_z}{\partial y})\\
&+\Re_\ell(E_{24}^1(\frac{\partial^2 w_s}{\partial y^2}+\frac{\partial^2\varphi_z}{\partial y^2})+E_{25}^1(\frac{\partial^2 w_s}{\partial x\partial y}+\frac{\partial^2\varphi_z}{\partial x\partial y})+A_{26}^1(\frac{\partial^2 u_0}{\partial y^2}+\frac{\partial^2 v_0}{\partial x\partial y})-2B_{26}^1\frac{\partial^3 w_b}{\partial x\partial y^2}-2C_{26}^1\\
&=\Re_\mu(I_0\frac{\partial^2 v_0}{\partial t^2}-I_1\frac{\partial^3 w_b}{\partial y\partial t^2}-J_1\frac{\partial^3 w_s}{\partial y\partial t^2})
\end{aligned}\tag{A2}$$

$$\begin{aligned}
&\Re_\ell(A_{11}^3\frac{\partial^3 u_0}{\partial x^3}-B_{11}^3\frac{\partial^4 w_b}{\partial x^4}-C_{11}^3\frac{\partial^4 w_s}{\partial x^4}+A_{12}^3\frac{\partial^3 v_0}{\partial x^2\partial y}-B_{12}^3\frac{\partial^4 w_b}{\partial x^2\partial y^2}-C_{12}^3\frac{\partial^4 w_s}{\partial x^2\partial y^2}+D_{13}^3\frac{\partial^2\varphi_z}{\partial x^2})\\
&+\Re_\ell(E_{14}^3(\frac{\partial^3 w_s}{\partial x^2\partial y}+\frac{\partial^3\varphi_z}{\partial x^2\partial y})+E_{15}^3(\frac{\partial^3 w_s}{\partial x^3}+\frac{\partial^3\varphi_z}{\partial x^3})+A_{16}^3(\frac{\partial^3 u_0}{\partial x^2\partial y}+\frac{\partial^3 v_0}{\partial x^3})-2B_{16}^3\frac{\partial^4 w_b}{\partial x^3\partial y}-2C_{16}^3\frac{\partial^4 w_s}{\partial x^3\partial y})\\
&+2\Re_\ell(A_{61}^3\frac{\partial^3 u_0}{\partial x^2\partial y}-B_{61}^3\frac{\partial^4 w_b}{\partial x^3\partial y}-C_{61}^3\frac{\partial^4 w_s}{\partial x^3\partial y}+A_{62}^3\frac{\partial^3 v_0}{\partial x\partial y^2}-B_{62}^3\frac{\partial^4 w_b}{\partial x\partial y^3}-C_{62}^3\frac{\partial^4 w_s}{\partial x\partial y^3}+D_{63}^3\frac{\partial^2\varphi_z}{\partial x\partial y})\\
&+2\Re_\ell(E_{64}^3(\frac{\partial^3 w_s}{\partial x\partial y^2}+\frac{\partial^3\varphi_z}{\partial x\partial y^2})+E_{65}^3(\frac{\partial^3 w_s}{\partial x^2\partial y}+\frac{\partial^3\varphi_z}{\partial x^2\partial y})+A_{66}^3(\frac{\partial^3 u_0}{\partial x\partial y^2}+\frac{\partial^3 v_0}{\partial x^2\partial y})-2B_{66}^3\frac{\partial^4 w_b}{\partial x^2\partial y^2}-2C_{66}^3\frac{\partial^4 w_s}{\partial x^2\partial y^2})\\
&+\Re_\ell(A_{21}^3\frac{\partial^3 u_0}{\partial x\partial y^2}-B_{21}^3\frac{\partial^4 w_b}{\partial x^2\partial y^2}-C_{21}^3\frac{\partial^4 w_s}{\partial x^2\partial y^2}+A_{22}^3\frac{\partial^3 v_0}{\partial y^3}-B_{22}^3\frac{\partial^4 w_b}{\partial y^4}-C_{22}^3\frac{\partial^4 w_s}{\partial y^4}+D_{23}^3\frac{\partial^2\varphi_z}{\partial y^2})\\
&+\Re_\ell(E_{24}^3(\frac{\partial^3 w_s}{\partial y^3}+\frac{\partial^3\varphi_z}{\partial y^3})+E_{25}^3(\frac{\partial^3 w_s}{\partial x\partial y^2}+\frac{\partial^3\varphi_z}{\partial x\partial y^2})+A_{26}^3(\frac{\partial^3 u_0}{\partial y^3}+\frac{\partial^3 v_0}{\partial x\partial y^2})-2B_{26}^3\frac{\partial^4 w_b}{\partial x\partial y^3}-2C_{26}^3\frac{\partial^4 w_s}{\partial x\partial y^3})\\
&=\Re_\mu(I_0(\frac{\partial^2 w_b}{\partial t^2}+\frac{\partial^2 w_s}{\partial t^2})+I_1(\frac{\partial^3 u_0}{\partial x\partial t^2}+\frac{\partial^3 v_0}{\partial y\partial t^2})-I_2\nabla^2\frac{\partial^2 w_b}{\partial t^2}-J_2\nabla^2\frac{\partial^2 w_b}{\partial t^2}+J_1^s\frac{\partial^2\varphi}{\partial t^2})
\end{aligned}\tag{A3}$$

$$
\begin{aligned}
&\Re_\ell(A_{11}^4\frac{\partial^3 u_0}{\partial x^3}-B_{11}^4\frac{\partial^4 w_b}{\partial x^4}-C_{11}^4\frac{\partial^4 w_s}{\partial x^4}+A_{12}^4\frac{\partial^3 v_0}{\partial x^2\partial y}-B_{12}^4\frac{\partial^4 w_b}{\partial x^2\partial y^2}-C_{12}^4\frac{\partial^4 w_s}{\partial x^2\partial y^2}+D_{13}^4\frac{\partial^2\varphi_z}{\partial x^2})\\
&+\Re_\ell(E_{14}^4(\frac{\partial^3 w_s}{\partial x^2\partial y}+\frac{\partial^3\varphi_z}{\partial x^2\partial y})+E_{15}^4(\frac{\partial^3 w_s}{\partial x^3}+\frac{\partial^3\varphi_z}{\partial x^3})+A_{16}^4(\frac{\partial^3 u_0}{\partial x^2\partial y}+\frac{\partial^3 v_0}{\partial x^3})-2B_{16}^4\frac{\partial^4 w_b}{\partial x^3\partial y}-2C_{16}^4\frac{\partial^4 w_s}{\partial x^3\partial y})\\
&+2\Re_\ell(A_{61}^4\frac{\partial^3 u_0}{\partial x^2\partial y}-B_{61}^4\frac{\partial^4 w_b}{\partial x^3\partial y}-C_{61}^4\frac{\partial^4 w_s}{\partial x^3\partial y}+A_{62}^4\frac{\partial^3 v_0}{\partial x\partial y^2}-B_{62}^4\frac{\partial^4 w_b}{\partial x\partial y^3}-C_{62}^4\frac{\partial^4 w_s}{\partial x\partial y^3}+D_{63}^4\frac{\partial^2\varphi_z}{\partial x\partial y})\\
&+2\Re_\ell(E_{64}^4(\frac{\partial^3 w_s}{\partial x\partial y^2}+\frac{\partial^3\varphi_z}{\partial x\partial y^2})+E_{65}^4(\frac{\partial^3 w_s}{\partial x^2\partial y}+\frac{\partial^3\varphi_z}{\partial x^2\partial y})+A_{66}^4(\frac{\partial^3 u_0}{\partial x\partial y^2}+\frac{\partial^3 v_0}{\partial x^2\partial y})-2B_{66}^4\frac{\partial^4 w_b}{\partial x^2\partial y^2}-2C_{66}^4\frac{\partial^4 w_s}{\partial x^2\partial y^2})\\
&+\Re_\ell(A_{21}^4\frac{\partial^3 u_0}{\partial x\partial y^2}-B_{21}^4\frac{\partial^4 w_b}{\partial x^2\partial y^2}-C_{21}^4\frac{\partial^4 w_s}{\partial x^2\partial y^2}+A_{22}^4\frac{\partial^3 v_0}{\partial y^3}-B_{22}^4\frac{\partial^4 w_b}{\partial y^4}-C_{22}^4\frac{\partial^4 w_s}{\partial y^4}+D_{23}^4\frac{\partial^2\varphi_z}{\partial y^2})\\
&+\Re_\ell(E_{24}^4(\frac{\partial^3 w_s}{\partial y^3}+\frac{\partial^3\varphi_z}{\partial y^3})+E_{25}^4(\frac{\partial^3 w_s}{\partial x\partial y^2}+\frac{\partial^3\varphi_z}{\partial x\partial y^2})+A_{26}^4(\frac{\partial^3 u_0}{\partial y^3}+\frac{\partial^3 v_0}{\partial x\partial y^2})-2B_{26}^4\frac{\partial^4 w_b}{\partial x\partial y^3}-2C_{26}^4\frac{\partial^4 w_s}{\partial x\partial y^3})\\
&+\Re_\ell(A_{51}^5\frac{\partial^2 u_0}{\partial x^2}-B_{51}^5\frac{\partial^3 w_b}{\partial x^3}-C_{51}^5\frac{\partial^3 w_s}{\partial x^3}+A_{52}^5\frac{\partial^2 v_0}{\partial x\partial y}-B_{52}^5\frac{\partial^3 w_b}{\partial x\partial y^2}-C_{52}^5\frac{\partial^3 w_s}{\partial x\partial y^2}+D_{53}^5\frac{\partial\varphi_z}{\partial x})\\
&+\Re_\ell(E_{54}^5(\frac{\partial^2 w_s}{\partial x\partial y}+\frac{\partial^2\varphi_z}{\partial x\partial y})+E_{55}^5(\frac{\partial^2 w_s}{\partial x^2}+\frac{\partial^2\varphi_z}{\partial x^2})+A_{56}^5(\frac{\partial^2 u_0}{\partial x\partial y}+\frac{\partial^2 v_0}{\partial x^2})-2B_{56}^5\frac{\partial^3 w_b}{\partial x^2\partial y}-2C_{56}^5\frac{\partial^3 w_s}{\partial x^2\partial y})\\
&+\Re_\ell(A_{41}^5\frac{\partial^2 u_0}{\partial x\partial y}-B_{41}^5\frac{\partial^3 w_b}{\partial x^2\partial y}-C_{41}^5\frac{\partial^3 w_s}{\partial x^2\partial y}+A_{42}^5\frac{\partial^2 v_0}{\partial y^2}-B_{42}^5\frac{\partial^3 w_b}{\partial y^3}-C_{42}^5\frac{\partial^3 w_s}{\partial y^3}+D_{43}^5\frac{\partial\varphi_z}{\partial y})\\
&+\Re_\ell(E_{44}^5(\frac{\partial^2 w_s}{\partial y^2}+\frac{\partial^2\varphi_z}{\partial y^2})+E_{45}^5(\frac{\partial^2 w_s}{\partial x\partial y}+\frac{\partial^2\varphi_z}{\partial x\partial y})+A_{46}^5(\frac{\partial^2 u_0}{\partial y^2}+\frac{\partial^2 v_0}{\partial x\partial y})-2B_{46}^5\frac{\partial^3 w_b}{\partial x\partial y^2}-2C_{46}^5\frac{\partial^3 w_s}{\partial x\partial y^2})\\
&=\Re_\mu(I_0(\frac{\partial^2 w_b}{\partial t^2}+\frac{\partial^2 w_s}{\partial t^2})+J_1(\frac{\partial^3 u_0}{\partial x\partial t^2}+\frac{\partial^3 v_0}{\partial y\partial t^2})-J_2\nabla^2\frac{\partial^2 w_b}{\partial t^2}-K_2\nabla^2\frac{\partial^2 w_b}{\partial t^2}+J_1^s\frac{\partial^2\varphi}{\partial t^2})
\end{aligned}
\tag{A4}
$$

$$
\begin{aligned}
&\Re_\ell(A_{51}^5\frac{\partial^2 u_0}{\partial x^2}-B_{51}^5\frac{\partial^3 w_b}{\partial x^3}-C_{51}^5\frac{\partial^3 w_s}{\partial x^3}+A_{52}^5\frac{\partial^2 v_0}{\partial x\partial y}-B_{52}^5\frac{\partial^3 w_b}{\partial x\partial y^2}-C_{52}^5\frac{\partial^3 w_s}{\partial x\partial y^2}+D_{53}^5\frac{\partial\varphi_z}{\partial x})\\
&+\Re_\ell(E_{54}^5(\frac{\partial^2 w_s}{\partial x\partial y}+\frac{\partial^2\varphi_z}{\partial x\partial y})+E_{55}^5(\frac{\partial^2 w_s}{\partial x^2}+\frac{\partial^2\varphi_z}{\partial x^2})+A_{56}^5(\frac{\partial^2 u_0}{\partial x\partial y}+\frac{\partial^2 v_0}{\partial x^2})-2B_{56}^5\frac{\partial^3 w_b}{\partial x^2\partial y}-2C_{56}^5\frac{\partial^3 w_s}{\partial x^2\partial y})\\
&+\Re_\ell(A_{41}^5\frac{\partial^2 u_0}{\partial x\partial y}-B_{41}^5\frac{\partial^3 w_b}{\partial x^2\partial y}-C_{41}^5\frac{\partial^3 w_s}{\partial x^2\partial y}+A_{42}^5\frac{\partial^2 v_0}{\partial y^2}-B_{42}^5\frac{\partial^3 w_b}{\partial y^3}-C_{42}^5\frac{\partial^3 w_s}{\partial y^3}+D_{43}^5\frac{\partial\varphi_z}{\partial y})\\
&+\Re_\ell(E_{44}^5(\frac{\partial^2 w_s}{\partial y^2}+\frac{\partial^2\varphi_z}{\partial y^2})+E_{45}^5(\frac{\partial^2 w_s}{\partial x\partial y}+\frac{\partial^2\varphi_z}{\partial x\partial y})+A_{46}^5(\frac{\partial^2 u_0}{\partial y^2}+\frac{\partial^2 v_0}{\partial x\partial y})-2B_{46}^5\frac{\partial^3 w_b}{\partial x\partial y^2}-2C_{46}^5\frac{\partial^3 w_s}{\partial x\partial y^2})\\
&-\Re_\ell(A_{31}^2\frac{\partial u_0}{\partial x}-B_{31}^2\frac{\partial^2 w_b}{\partial x^2}-C_{31}^2\frac{\partial^2 w_s}{\partial x^2}+A_{32}^2\frac{\partial v_0}{\partial y}-B_{32}^2\frac{\partial^2 w_b}{\partial y^2}-C_{32}^2\frac{\partial^2 w_s}{\partial y^2}+D_{33}^2\varphi_z)\\
&-\Re_\ell(E_{34}^2(\frac{\partial w_s}{\partial y}+\frac{\partial\varphi_z}{\partial y})+E_{35}^2(\frac{\partial w_s}{\partial x}+\frac{\partial\varphi_z}{\partial x})+A_{36}^2(\frac{\partial u_0}{\partial y}+\frac{\partial v_0}{\partial x})-2B_{36}^2\frac{\partial^2 w_b}{\partial x\partial y}-2C_{36}^2\frac{\partial^2 w_s}{\partial x\partial y})\\
&=\Re_\mu(J_1^s(\frac{\partial^2 w_b}{\partial t^2}+\frac{\partial^2 w_s}{\partial t^2})-K_2^s\frac{\partial^2\varphi_z}{\partial t^2})
\end{aligned}
\tag{A5}
$$

in which

$$\begin{bmatrix} A_{ij}^1 & B_{ij}^1 & C_{ij}^1 & D_{ij}^1 & E_{ij}^1 \\ A_{ij}^2 & B_{ij}^2 & C_{ij}^2 & D_{ij}^2 & E_{ij}^2 \\ A_{ij}^3 & B_{ij}^3 & C_{ij}^3 & D_{ij}^3 & E_{ij}^3 \\ A_{ij}^4 & B_{ij}^4 & C_{ij}^4 & D_{ij}^4 & E_{ij}^4 \\ A_{ij}^5 & B_{ij}^5 & C_{ij}^5 & D_{ij}^5 & E_{ij}^5 \end{bmatrix} = \int_{-h/2}^{h/2} Q_{ij} \begin{bmatrix} 1 & z & f & g' & g \\ g' & zg' & fg' & g'g' & gg' \\ z & z^2 & fz & g'z & gz \\ f & zf & f^2 & g'f & gf \\ g & gz & gf & gg' & g^2 \end{bmatrix} dz; \quad (i,j) = (1,2,...6) \tag{A6}$$